Identification of *NSDHL* mutations associated with CHILD syndrome in oral verruciform xanthoma

George I. Getz, DDS, MS,[a] Kshitij Parag-Sharma, BA,[b] Jonathan Reside, DDS, MS,[c] Ricardo J. Padilla, DDS,[d] and Antonio L. Amelio, PhD[e]

Objective. The aim of this study was to perform a systematic analysis of the nicotinamide adenine dinucleotide phosphate (NAD[P])−dependent steroid dehydrogenase-like (*NSDHL*) gene in cases of oral verruciform xanthoma (VX) and to test for the presence of mutations associated with congenital hemidysplasia with ichthyosiform nevus and limb defects (CHILD) syndrome.

Study Design. DNA was extracted from archived paraffin-embedded tissue of oral VX and control cases. Polymerase chain reaction (PCR) was then used to screen exons 4 and 6 of the *NSDHL* gene for the presence of 4 known germline mutations associated with CHILD syndrome and 1 somatic mutation previously identified in VX lesions with no known association with CHILD syndrome.

Results. Of the 16 oral VX tissue samples, 8 (50%) had known missense mutations associated with CHILD syndrome. Furthermore, 2 of these 8 tissue samples also had an additional missense mutation previously identified in cutaneous VX lesions. No mutations of exons 4 and 6 were found in the 5 negative control tissue samples.

Conclusions. *NSDHL* gene mutations associated with CHILD syndrome are common in sporadic oral VX cases, suggesting that these mutations confer a greater risk for the development of epithelial barrier defects that promote recurrent oral VX lesions and the potential for direct germline transmission of oral VX susceptibility. (Oral Surg Oral Med Oral Pathol Oral Radiol 2019;128:60−69)

Verruciform xanthoma (VX) primarily affects the oral mucosa and commonly presents as well-circumscribed verrucous or papillomatous lesions, although it can also appear flat, polypoid, or sessile.[1] In a study of a multifocal VX in the upper aerodigestive tract of a child, 3 morphologic manifestations of VX (verruciform, papillary, and flat) were identified within the same individual. This suggested that the squamous epithelium progresses through flat and papillary stages, before becoming verrucous.[2] Oral VX lesions are often small (2 mm−2 cm), solitary, asymptomatic, slow growing, white, pink, gray, or yellowish lesions.[3] VX lesions occur most commonly on the gingiva (40.9%−70.6%) but have also been found on the mandibular ridge, palate, floor of the mouth, lip, and mucobuccal fold.[1,3,4] Additionally, VX lesions have also been identified on the faucial pillars and the upper respiratory tract.[2,5] Excisional biopsy followed by histologic evaluation is the primary means of diagnosis. The differential diagnosis for oral VX may include squamous papilloma, verruca vulgaris, condyloma acuminatum, verrucous hyperkeratosis, and other mucosal lesions that induce texture changes to the epithelial surface.[6] Treatment via excision is usually curative for oral VX lesions because recurrence is rare[7]; only 3 cases of recurrence have ever been described, and in all of them, the lesions were localized to the hard palate.[8] In contrast, a higher recurrence has been reported for cutaneous VX, although the condition resolves eventually.[9]

The etiology and pathogenesis of oral VX is currently unknown. The verruciform or papillary nature of VX lesions in the oral cavity and genitalia has suggested the potential for human papilloma virus (HPV) involvement in the etiology of this disease.[10] In fact, HPV DNA was detected in a condyloma-appearing VX, and 1 case report identified HPV type 6a particles in the nucleus of keratinocytes from a cutaneous VX (scrotum) lesion after polymerase chain reaction (PCR) and sequence analysis.[11,12] However, no signs of HPV infection have ever been detected, and multiple studies have failed to prove a causal connection to VX.[10] However, a hallmark of VX is the presence

Statement of Clinical Relevance

Mutations of the *NSDHL* gene known to be associated with congenital hemidysplasia with ichthyosiform nevus and limb defects syndrome have been identified in oral verruciform xanthoma lesions. These findings support a genetic basis for oral verruciform xanthoma etiology and raise the question of potential genetic transmission of disease risk.

[a]Department of Periodontology, UNC School of Dentistry, University of North Carolina at Chapel Hill, Chapel Hill, NC, USA.
[b]Graduate Curriculum in Cell Biology & Physiology, Biological & Biomedical Sciences Program, UNC School of Medicine, University of North Carolina at Chapel Hill, Chapel Hill, NC, USA.
[c]Department of Periodontology, UNC School of Dentistry, University of North Carolina at Chapel Hill, Chapel Hill, NC, USA.
[d]Department of Diagnostic Sciences, UNC School of Dentistry, University of North Carolina at Chapel Hill, Chapel Hill, NC, USA.
[e]Departments of Oral and Craniofacial Health Sciences and Dental Ecology, UNC School of Dentistry, Chapel Hill, NC, USA; Lineberger Comprehensive Cancer Center, UNC School of Medicine, Chapel Hill, NC, USA.
Received for publication Oct 9, 2018; returned for revision Jan 4, 2019; accepted for publication Feb 15, 2019.

2212-4403/$-see front matter
https://doi.org/10.1016/j.oooo.2019.02.015

of foamy (lipid-laden) histiocytes, or xanthoma cells, within the connective tissue papillae between rete ridges. The origins of the xanthoma cells remain unclear, but it has been proposed that these cells arise from epithelial degradation in a process whereby the epithelium becomes entrapped within the "crypts" of the stratified squamous epithelium, the cell membranes then degenerate, and eventually accumulate the lipid characteristic of foam cells.[13] Foamy histiocytes are seen in many conditions where macrophages are involved in phagocytizing lipids and cell membrane byproducts. The products of this breakdown elicit an inflammatory response that leads to neutrophil infiltrates often seen within the epithelium and a mostly chronic inflammatory cell infiltrate in the submucosa.[13] It is unclear, however, how the initial "crypt" that would necessitate the entrapment of epithelial cells forms, although it is proposed that it may be caused by trauma secondary to a local irritant.[10] Later studies, however, found foam cell deposition in areas of little epithelial degradation and without entrapment of epithelial cells.[2] Given that macrophages are known to produce a variety of growth factors,[14] it has been suggested that the foam cells may play a role in inducing epithelial hyperplasia. Therefore, it is believed that the accumulation of foam cells is the primary abnormality in the early lesion and that increasing epithelial hyperplasia and inflammation are secondary manifestations.[2]

Recently, cutaneous VX was found associated with the X-linked autosomal dominant lipid storage disease Congenital hemidysplasia with ichthyosiform erythroderma and limb defects (CHILD) caused by a mutation of the nicotinamide adenine dinucleotide phosphate (NAD[P]) steroid dehydrogenase-like (*NSDHL*) gene required for cholesterol biosynthesis.[10] The lesions in CHILD syndrome and cutaneous VX have similar morphologic and histologic appearances, including the presence of foam cells confined to the connective tissue papillae. Thus, the purpose of this study was to investigate potential associations between the presence of inactivating mutations in the *NSDHL* gene and sporadic oral VX.

MATERIALS AND METHODS

Archived samples collection

This project's protocol was reviewed and approved by the Institutional Review Board of the University of North Carolina (UNC) at Chapel Hill (protocol No. 16-1270). After approval, the archives of the UNC Oral and Maxillofacial Biopsy Service were searched for cases of oral VX. Twenty-five formalin-fixed, paraffin-embedded (FFPE) tissue blocks were retrieved from the UNC Oral Pathology Laboratory and Biopsy Service by using consecutive sampling. The accession dates ranged from July 2015 to December 2017. Twenty of the test samples had been previously diagnosed as oral VX, and 5 samples that had been diagnosed as oral mucoceles served as negative controls. Mucoceles were selected as controls because in that condition, the epithelium is usually only minimally irritated. Furthermore, although mucoceles also contain foamy histiocytes (a hallmark of VX lesions) surrounding the mucous pool, mucoceles are not associated with *NSDHL* mutations. Despite access to additional oral VX cases in our archives, limited funding restricted the number of cases analyzed in this study. All cases were diagnosed by a board-certified oral and maxillofacial pathologist and subsequently confirmed by one of the authors of this article (R.J.P., a board-certified oral and maxillofacial pathologist). Each sample came from a unique human subject. The tissue blocks were deidentified and assigned a study number. Clinical data of those cases were collected under the study number. No patient identifiers were collected or kept.

DNA extraction from samples

Five tissue sections (5 μm thick) were produced using a microtome from each selected FFPE block. Each sample was deparaffinized with one 1-mL wash of 100% xylene followed by one 1-mL wash in 100% ethanol. The deparaffinized tissues were then subjected to DNA extraction with the EX-WAX paraffin-embedded DNA extraction kit (Millipore Sigma, Darmstadt, Germany), according to the manufacturer's instructions. DNA concentrations at 260/280 and 260/230 ratios (see Supplementary Table S1) were assessed by using a DeNovix DS-11 spectrophotometer (DeNovix, Wilmington, DE). All DNA samples and their dilutions were stored at −20°C.

Plasmid construction

A plasmid was designed and subsequently constructed by Invitrogen GeneArt Synthesis (Thermo Fisher Scientific, Regensburg, Germany) to include mutations of interest previously reported in the literature from exon 4 and exon 6 of the *NSDHL* (NM_015922.2), including C>T = A105 V within Exon 4 and G>C = A182 *P*, G>A = R199 H, and G>A = G205 S within exon 6 (see Supplemental Figure S1). G>A = R199 H was associated with a somatic mutation found in VX tissues, and the others have been reported as being associated with CHILD syndrome[10]. The synthesized *NSDHL* fragment (1131 base pairs [bp]) containing the mutations was cloned into the pcDNA3.1_V5-HistA_A122 vector; then, 5 μg of the lyophilized DNA was dissolved in 50 μL of distilled water. Transformation was accomplished with DH5-alpha competent cells (Thermo Fisher Scientific, Durham, NC) according to the manufacturer's instructions. After overnight incubation at 37°C, the plasmid was recovered by using the NucleoSpin Plasmid miniprep kit (Macherey-Nagel GmbH & Co., Duren, Germany). The plasmid and its dilution to a 37.5 ng/μL concentration were stored at −20°C. The plasmid, including the

mutations of interest, was constructed for comparison with test samples after being spiked into a control sample. This combination served as the positive control.

PCR amplification of exons 4 and 6 of the *NSDHL* gene

Primer sets were designed to amplify mutations reported in the literature within exons 4 and 6 of the *NSDHL* gene (Eton Biosciences, Research Triangle Park, NC)[10]. These include C>T = A105 V within exon 4, as well as G>C = A182 P; G>A = R199 H; G>A = G205 S; and C>T = Q210 X within exon 6. The primer sequences were 5'-CCA GCT CTG AAA GGT GTA AAC ACA-3' (sense) and 5'-CAA GTT TCA ATG ACA TTC TTG GTG CC-3' (antisense) for exon 4; and 5'-A GTT CTG GGC GCC AAC GAT-3' (sense) and 5'-CAA TCA CGA ACT TCA TCT TGC CGT-3' (antisense) for exon 6. We later designed an additional primer—an intron 5 primer (5' - GCA CTC TCT TGG CTT GGG-3' (sense))—to pair with the previously described exon 6 (antisense) primer to capture an additional mutation described in the literature for CHILD syndrome— G>C = A182 P.[10] The positive control plasmid itself was verified via amplification with the exon 4 F/R, exon 6 F/R, and the exon 4 F/6 R primer sets (amplicon sizes of 119, 140, 409 bp, respectively) and this was followed by Sanger sequencing. The size of PCR amplicons expected from the test and control samples was 119 bp for exon 4 sense/antisense primers; 140 bp for exon 6 sense/antisense primers; and 206 bp for intron 5 sense/exon 6 antisense primers. All PCR products were verified via visualization by electrophoresis on 1.5% agarose gels by using either genomic HEK293 T DNA or control plasmid DNA templates.

Each amplification was carried out in a Bio-Rad T100 Thermal Cycler (Bio-Rad Laboratories, Hercules, CA) in a 50-μL PCR mixture containing 600 ng genomic DNA; 5 μL(50 μM) of each sense and antisense primer; 25 μL Maxima Hot Start PCR Master Mix (2 X) (composition: 400 μM deoxyadenosine triphosphate, 400 μM deoxyguanosine triphosphate, 400 μM deoxycytidine triphosphate, 400 μM deoxythymidine triphosphate, 4 mM magnesium chloride, Maxima Hot Start Taq DNA polymerase in 2 X PCR buffer [Thermo Fisher Scientific, Durham, NC]); and DNase/RNase-free distilled water.

The 16 test samples (designated T1−T16) and the 5 negative controls (designated C1−C5) were amplified with exon 4 primer pairs, the exon 6 primer pairs, and the intron 5/exon 6 (antisense) primer pairs. The positive control plasmid was amplified with exon 4 sense and exon 6 antisense primers. As mentioned previously, one of the control samples (C5) spiked with the plasmid (C5-PL) and amplified with the same primer pairs served as positive control. Thermocycling conditions used were initial denaturation and hot start at 95°C for 15 minutes; 40 cycles consisting of 30 seconds at 95°C; 30 seconds at 60°C; and then 1 minute at 72°C. After thermocycling, reactions were subjected to 72°C incubation for 5 minutes. PCR amplicons were visualized by electrophoresis on 2% agarose gels and with Gel Red (Biotium, Fremont, CA) staining. After ultraviolet transillumination, selected bands corresponding to the aforementioned bp length (verified via molecular-weight size marker) were incised from the agarose gels for purification.

PCR purification and sanger sequencing of PCR amplicons

The agarose gel sections containing the amplified PCR products were purified by using the NucleoSpin Gel and PCR Clean-up kit (Macherey-Nagel GmbH & Co., Duren, Germany). DNA was sequenced by using a DNA sequencer (model 377; Applied Biosystems, Foster City, CA) as previously described (Eton Bioscience, Research Triangle Park, NC). The DNA templates used for the sequencing were at concentrations of 10 to 30 ng/μL.

Analysis of Sanger sequencing

Reference sequences were obtained from GenBank (NCBI reference sequence NM_015922.2) for the human *NSDHL* cDNA sequence and the mutant *NSDHL* cDNA sequence, which contained the mutations of interest. Consensus alignments and analysis of the sequencing results were performed by using Molecular Biology 2.0 software (Benchling, San Francisco, CA). Separate consensus alignments were used for the exon 4 and exon 6 amplicons. Mutations were analyzed to determine whether any amino acid change (or stop codon) resulted from the base pair change. Chromatograms were visualized by using the FinchTV (version 1.5.0) software. Consensus multiple sequence alignment figures were created from relevant chromatograms by using the Multalin software (http://multalin.toulouse.inra.fr/multalin/).

RESULTS

To study the etiology and pathogenesis of oral VX, we identified a cohort of patients with clinical impressions with the potential to overlap with a differential diagnosis that would include oral VX, in addition to a cohort of patient controls (Figure 1 and Table I). Mean age of patients with oral VX was 61.5 years (range 15−92 years), and mean age of the control patients was 25 years (range 10−39 years). Of note, the mucocele controls also contained foamy histiocytes (a hallmark of VX lesions) surrounding the mucous pool but were not associated with *NSDHL* mutations. For the test group, 68.8% of the oral VX lesions were found in females (11 of 16), and 60% (3 of 5) patients in the control group were females. The most common clinical impressions submitted with biopsy specimens for the oral VX lesions were dysplasia, papilloma, and squamous cell carcinoma. Interestingly, patients with

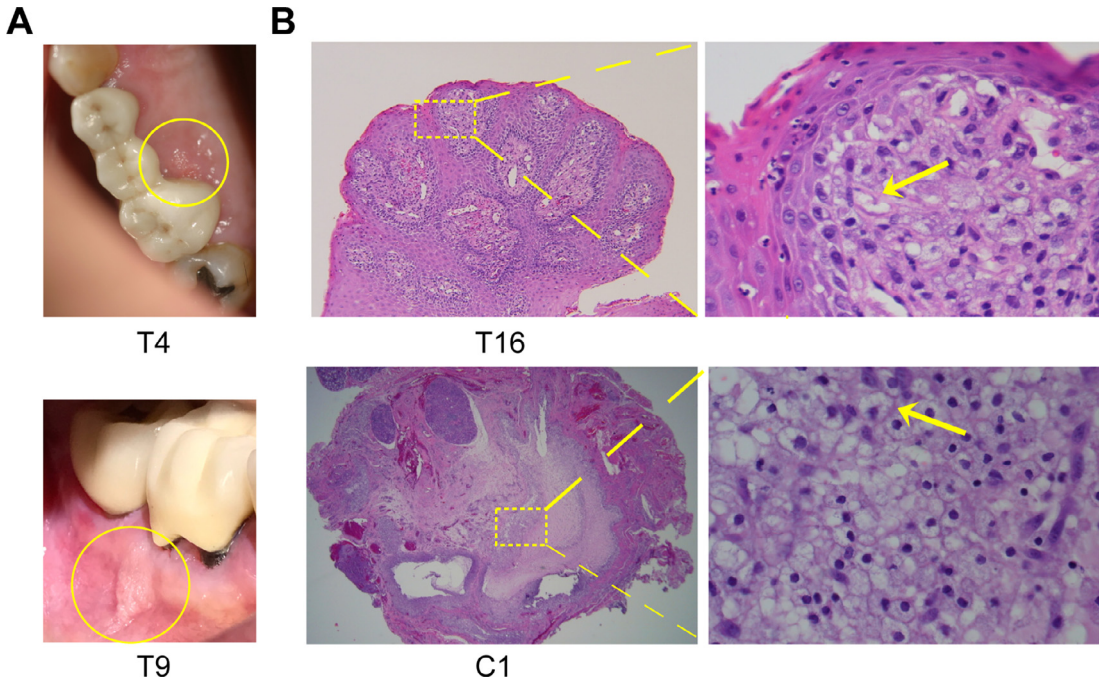

Fig. 1. Representative images of oral verruciform xanthoma cases selected. **(A)** Clinical presentation of verruciform xanthoma (VX) for cases T4 and T9. Most lesions will have a cobblestone-like surface architecture and vary in color from pink-red to white-yellow. Attached keratinized gingiva and palate are common places to encounter oral VX. **(B)** Histopathology. Case T16 exhibits oral VX with a mildly undulated surface architecture of the epithelium, with mild hyperkeratosis and an orange hue. Abundant foamy histiocytes are seen in the connective tissue between the epithelial rete pegs and below the epithelium. The higher-magnification area shows more detail of the foamy nature of the cytoplasm of the histiocytes *(yellow arrow)*. Case C1 is a representative mucocele control that exhibits variably sized foamy histiocytes *(yellow arrow)* containing mucinous secretions produced by the minor salivary gland associated with the mucocele.

CHILD syndrome commonly display unilateral disease manifestation on the right side of the body because of mosaic X chromosome inactivation/lyonization.[15] In our study, 75% (12 of 16) of the oral VX test samples were listed as coming from the right side of the mouth (although the side of one of the remaining samples was not specified, and 2 were from the midline, encompassing both the left and right sides).

To investigate the connections between oral VX and the *NSDHL* mutations associated with CHILD syndrome, we used PCR primer pairs that generated amplicons within the exon−exon boundaries from processed *NSDHL* mRNA (Figure 2A) or an intron−exon boundary from unspliced *NSDHL* mRNA (not illustrated) that encompassed known *NSDHL* mutations. Successful PCR amplification of the Ex4, Ex6, and Int5 F/Ex6 R primer combinations was confirmed with PCR by using HEK293 T genomic DNA as a template (Figure 2B). A plasmid control was also designed to harbor all currently known *NSDHL* mutations within exons 4 and 6, and successful PCR amplification of the Ex4, Ex6, and Ex4 F/Ex6 R primer combinations were confirmed by using this plasmid DNA as a template (see Supplemental Figure S1; Figure 2C). Differences in the archived samples with regard to date of fixation, duration of fixation, and efficiency of deparaffinization influenced the extraction and optimization of some samples; however, 16 samples from the original 20 tissue samples selected for this study successfully yielded high-quality DNA (labeled T1−T16; Table II). Of note, DNA was successfully extracted from all of the original 5 control samples (C1−C5). *NSDHL* mutations in the plasmid DNA control were validated by using Sanger sequencing of the predicted PCR amplicons (Figure 3A). To confirm the ability to amplify and detect *NSDHL* mutations within DNA isolated from archived FFPE tissue samples, this plasmid was spiked into the control (C5) tissue sample, and amplicons generated from exon 4 were subjected to sequencing (Figure 3B). Notably, analysis of the sequencing chromatograms reveals the ability to discriminate both wild-type and mutant alleles, indicating that successful detection of a heterozygous genotype is possible.

Analysis of oral VX lesion sequence alignments revealed that 50% (8 of 16) test cases harbored mutations within *NSDHL* exon 4, which previously had been reported for CHILD syndrome (Figure 4A). Two of these 8 lesions had a homozygous, c.314 (C>T) missense mutation at codon 105 (GCG>GTG), which results in replacement of the amino acid alanine by valine (A105 V) in the

Table I. Clinicopathologic characteristics of patient samples

Sample	*Age/sex*	*Anatomic location*	*Clinical impression(s)*
C1	28/M	Right lower lip	Mucocele
C2	39/M	Right lower lip	Mucocele, fibroma
C3	17/F	Lower lip (Side unspecified)	Mucocele, fibroma
C4	31/F	Right lower lip	Mucocele
C5	10/F	Lower lip (Side unspecified)	Mucocele, fibroma
T1	67/M	Right retromolar pad	Verrucous hyperplasia, papilloma, squamous cell carcinoma
T2	89/M	Right mandibular buccal attached gingiva (Tooth #30)	Leukoplakia
T3	63/F	Right posterior mandibular buccal vestibule	Verrucous hyperplasia, papilloma, squamous cell carcinoma
T4	92/F	Right palatal (Tooth #3)	Fibroma
T5	42/F	Right palatal (Tooth #3)	Not provided
T6	70/M	Right buccal mucosa (Arch unspecified)	Not provided
T7	59/F	Right palatal (Tooth #3)	Papilloma
T8	76/F	Palate (Side unspecified)	Irritation fibroma
T9	81/F	Left buccal mucosa (Tooth #19)	Epithelial dysplasia
T10	62/M	Midline mandibular lingual (Teeth #24,25)	Verruciform xanthoma
T11	69/F	Right buccal mucosa	Dysplasia, squamous cell carcinoma
T12	56/F	Right lateral of tongue	Papilloma
T13	43/F	Right (buccal or palatal not specified) (Tooth #2)	Hyperkeratosis, dysplasia
T14	45/F	Right mandibular buccal mucosa (Tooth #31)	HPV lesion
T15	55/F	Teeth #24,25 (Buccal/lingual gingiva unspecified)	"Wart"
T16	15/M	Right maxillary buccal papilla (Teeth #6/7)	Not provided

final protein product. The remaining 6 lesions had heterozygous missense mutations, which included the same nucleotide substitution as the homozygous mutations (GCG>GTG) (see Supplemental Figure 2A). Neither the A105 V mutation nor any other mutation was found in any of the remaining 8 oral VX lesions or in any of the 5 control samples.

With respect to exon 6, 2 (12.5%) of the oral VX lesions harbored multiple mutations (Figure 4B). One of the mutations has previously been reported for CHILD syndrome, and the other was a mutation previously reported in the literature to be associated with cutaneous VX.[10] Both the T4 and T16 samples harbored a heterozygous, c.613 (G>A) missense mutation at codon 205 (GGC>AGC) that results in the replacement of the amino acid glycine by serine (G205S) in the final protein product (see Supplemental Figure 2B). This mutation was of interest because of its known association with CHILD syndrome. Additionally, each of the 2 lesions had a heterozygous, c.596 (G>A) missense mutation at codon 199 (CGC>CAC), which results in the replacement of the amino acid arginine by histidine (R199H) in the final protein product (see Figure 4B and Supplemental Figure 2B). This mutation was previously reported in 2 cutaneous VX lesions but is not known to be associated with CHILD syndrome.[10] These same 2 oral VX lesions were also identified as harboring A105 V exon 4 mutations (see Figure 4A). Neither the A205 V or R199H mutation nor any other mutation was found in any of the remaining 14 oral VX lesions or in any of the 5 control samples. Additionally, neither of the other mutations of interest (A182P or Q201X) was found in any of the oral VX lesion or control samples. *NSDHL* mutational status across all samples analyzed for this study are summarized in Table II.

DISCUSSION

Published evidence suggests that the characteristic lesions found in CHILD syndrome, with their similar clinical and histologic presentations, are strongly related to VX.[16] We confirm that *NSDHL* mutations present in CHILD syndrome lesions are associated with mutations observed in oral VX lesions. The ages of test patients found to harbor *NSDHL* mutations ranged from 15 to 92 years (mean age 61.5 years). Discounting test sample 16 from a 15-year old male patient, the age range in our study was 43 to 92 years (mean age 64.6 years). Notably, except the 15-year-old male, all the heterozygous *NSDHL* mutations that we identified were derived from female patients. Both homozygous mutations were found in 67- and 89-year old men. Unfortunately, a complete health history was not available for any of the patients. Thus, it is not known whether patients had a personal or family history of CHILD syndrome, and this limited our ability to draw conclusions about direct germline transmission of oral VX susceptibility.

The *NSDHL* gene was only discovered within the last 15 years and encodes a 3 β-hydroxysteroid dehydrogenase that regulates a rate-limiting step of cholesterol biosynthesis. It is believed that a nonfunctional NSDHL

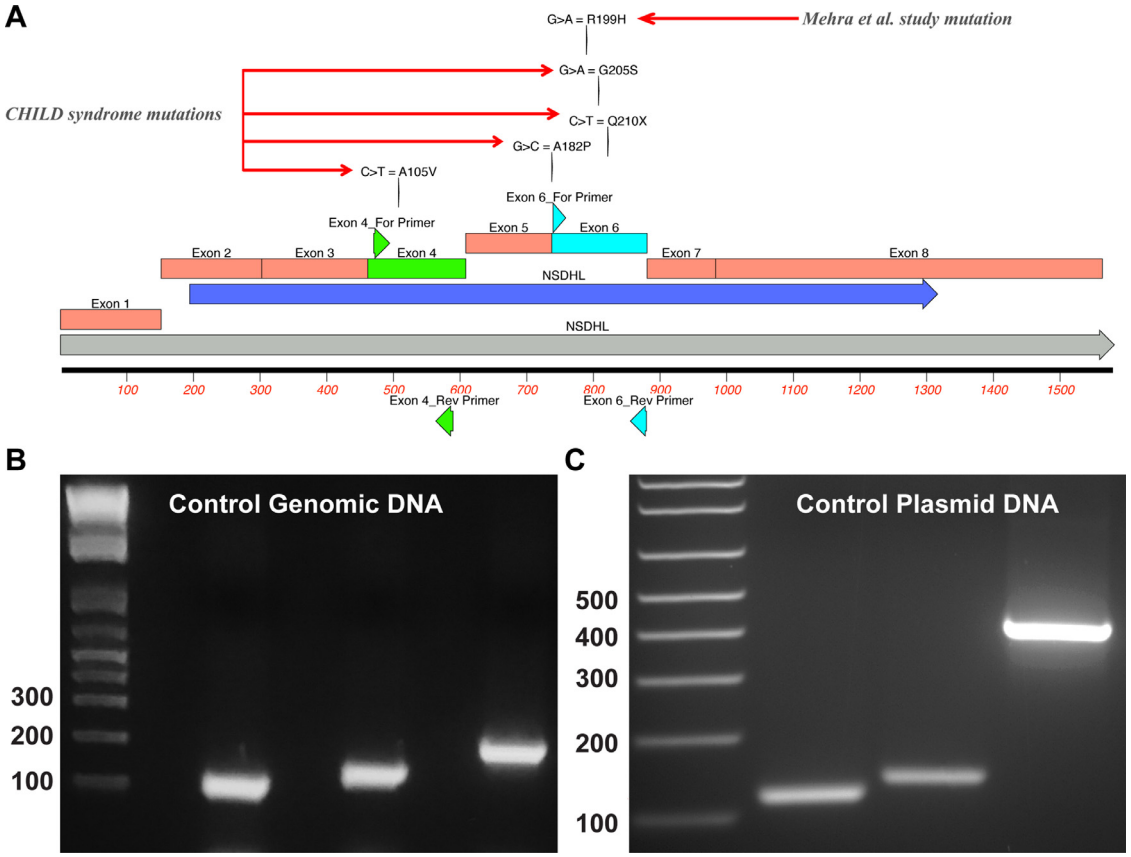

Fig. 2. Illustration and validation of *NSDHL*-derived polymerase chain reaction (PCR) amplicons. **(A)** Diagram of the *NSDHL* mRNA transcript *(gray)* with exons 1 through 8 highlighted independently of the open reading frame *(blue)*. Previously described mutations, including 4 germline mutations associated with CHILD syndrome in exon 4 and exon 6 and 1 somatic mutation not known to be associated with CHILD syndrome in exon 6, are annotated relative to the forward and reverse primers locations (*Note:* Introns are not depicted; therefore, the forward Intron 5 F primer is not annotated). **(B)** Representative agarose gel confirming PCR amplicon sizes with use of HEK293 T genomic DNA. Expected sizes: Lane 1: 119 bp *NSDHL* exon 4 F/R; lane 2: 140 bp *NSDHL* exon 6 F/R; and lane 3: 206 bp *NSDHL* Intron 5 F/exon 6 R. **(C)** Representative agarose gel confirming PCR amplicon sizes with use of the mutant plasmid DNA. Expected sizes: Lane 1: 119 bp *NSDHL* exon 4 F/R; lane 2: 140 bp *NSDHL* exon 6 F/R; and lane 3: 409 bp *NSDHL* exon 4 F/exon 6 R.

enzyme may cause the characteristic VX lesions of CHILD syndrome, through the absence of cholesterol, other downstream sterols, or a buildup of intermediate NSDHL-mediated upstream byproducts.[17] These abnormalities in cholesterol biosynthesis are thought to prevent the establishment and upkeep of a complete cutaneous or epithelial barrier because cholesterol is a major precursor of steroid hormones influencing embryonic and postnatal development and is a vital component of cell membranes. The NSDHL protein is found within the membranes of the endoplasmic reticulum and on the surface of intracellular lipid storage droplets.[18] It has been reported that instead of just serving as a vessel for lipid storage, the droplets themselves may be involved in the regulation of cholesterol biosynthesis. Normally, NSDHL migrates from the endoplasmic reticulum to lipid droplets and initiates a negative feedback to stop lipid droplet production if an adequate amount of lipid droplets have been produced for the local environment. However, introduction of the missense mutation found in CHILD syndrome (G205S, a mutation also detected in our study) into the *NSDHL* gene renders the encoded enzyme inactive, and negative feedback is lost, resulting in increased lipid droplet synthesis[18] and potentially accounting for the foam cells that are the hallmark of VX lesions.

In humans, one of the X chromosomes in females is silenced at random with regard to its parental origin, a process termed *X-inactivation*. This randomization occurs early in embryonic development and is maintained through all cell divisions. X-inactivation occurs in every female and consists of a mosaic of cell populations, where either the paternal or maternal derived X-chromosome has been inactivated.[19] X-linked diseases, such as CHILD syndrome, are overwhelmingly lethal in males because they have only one X-chromosome, whereas the mosaicism of X-inactivation in females is often protective in case of heterozygous

Table II. Summary of *NSDHL* mutational status across patient samples

Sample	*Mutations*		*Nucleotide affected*	*Type of mutation(s)*	*Resultant AA change*	*Associated mutation*	
	Exon 6	*Exon 4*				*Cutaneous VX*	*CHILD syndrome*
C1	—	—	—	—	—	—	—
C2	—	—	—	—	—	—	—
C3	—	—	—	—	—	—	—
C4	—	—	—	—	—	—	—
C5	—	—	—	—	—	—	—
T1	—	YES	c.314	C>T*	Alanine>Valine	—	YES
T2	—	YES	c.314	C>T*	Alanine>Valine	—	YES
T3	—	—	—	—	—	—	—
T4	YES	YES	c.314	C>T	Alanine>Valine	—	YES
			c.596	G>A	Arginine>Histidine	YES	—
			c.613	G>A	Glycine>Serine	—	YES
T5	—	—	—	—	—	—	—
T6	—	—	—	—	—	—	—
T7	—	—	—	—	—	—	—
T8	—	YES	c.314	C>T	Alanine>Valine	—	YES
T9	—	YES	c.314	C>T	Alanine>Valine	—	YES
T10	—	—	—	—	—	—	—
T11	—	—	—	—	—	—	—
T12	—	—	—	—	—	—	—
T13	—	—	—	—	—	—	—
T14	—	YES	c.314	C>T	Alanine>Valine	—	YES
T15	—	YES	c.314	C>T	Alanine>Valine	—	YES
T16	YES	YES	c.314	C>T	Alanine>Valine	—	YES
			c.596	G>A	Arginine>Histidine	YES	—
			c.613	G>A	Glycine>Serine	—	YES

*Homozygous mutation.
CHILD, congenital hemidysplasia with ichthyosiform nevus and limb defects, *VX,* verruciform xanthoma.

mutations. As expected, a more variable phenotype is usually seen in females, with heterozygous carriers displaying mild symptoms.[20] As anticipated, CHILD syndrome in males are extremely rare because of the X-linked autosomal dominant nature of this disease, and only 1 case has been documented. This male patient had an otherwise normal karyotype but was heterozygous for "wild type" and mutant alleles in cultured fibroblasts from affected cutaneous lesions, suggesting that the mutation represented an early postzygotic event. As in CHILD syndrome, the majority of our study lesions that possessed mutations were located on the right side of the subject (5 of 8, with 2 of the other 8 samples presenting at the midline, and 1 on the left side) (see Table I). In CHILD syndrome, this variability and the common clinical presentation primarily on one side of the body (prevalence for the right side)[15] has been explained as being caused by mosaicism of X-inactivation/lyonization.[21] To our knowledge, there is no documented correlation of gender and/or body axis predilection with the development of oral VX lesions. However, it is tempting to speculate that *NSDHL* is involved in regulating the normal establishment of left−right body symmetry and that inherited germline *NSDHL* mutations are lethal embryonically if specifically expressed during left axis organogenesis. However, although it is tempting to make direct comparisons between patients diagnosed with CHILD syndrome and our patients with oral VX, it is important to note that no germline testing was conducted for any of the patients from whom we derived tissue samples.

In our study, the only homozygous mutations (C>T at codon 105) were found in males, except for test sample 16 (T16), which unexpectedly presented with heterozygous mutations in both exon 4 and exon 6. In the absence of any follow-up clinical information, it remains plausible that patient T16 is, in fact, female and/or has a gender neutral name. In our test samples, 8 samples (50%) displayed either a homozygous or a heterozygous mutation at codon 105 (GCG>GTG), resulting in a replacement of alanine with valine in the final protein product (A105V). Two samples displayed a heterozygous mutation at codon 205 (GGC>AGC), resulting in replacement of alanine by serine in the final protein product (G205S). These 2 different missense mutations are found in patients diagnosed with CHILD syndrome. These same 2 test samples also displayed a heterozygous mutation at codon 199 (CGC>CAC), resulting in a replacement of arginine by histidine in the final protein product (R199H). This is the same novel somatic missense mutation encountered in the Mehra et al. study. It is notable that these 2 test samples were also included in the 8 test samples that had a mutation at codon 105. The other mutations of interest for our study in exon 6 that have been

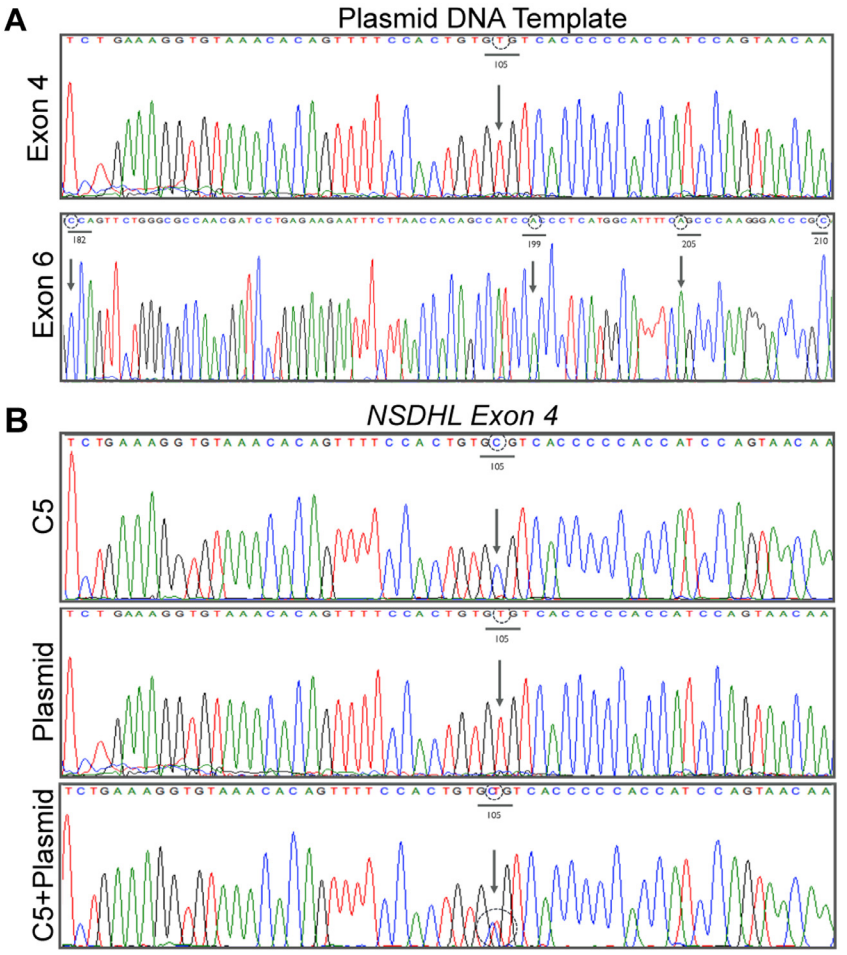

Fig. 3. Representative Sanger sequencing results for **(A)** exon 4 and exon 6 from plasmid DNA that contains the mutant *NSDHL* template, and **(B)** comparisons of exon 4 from a control sample (C5), plasmid DNA alone, or control sample spiked with the mutant plasmid DNA (C5 + plasmid). The chromatograms reveal the locations of missense mutations at nucleotides mapping within codons 105 (C>T, A105V), 182 (G>C, A182*P*), 199 (G>A, R199H), and 205 (G>A, G205S) or the nonsense mutation at 210 (C>T, Q210X).

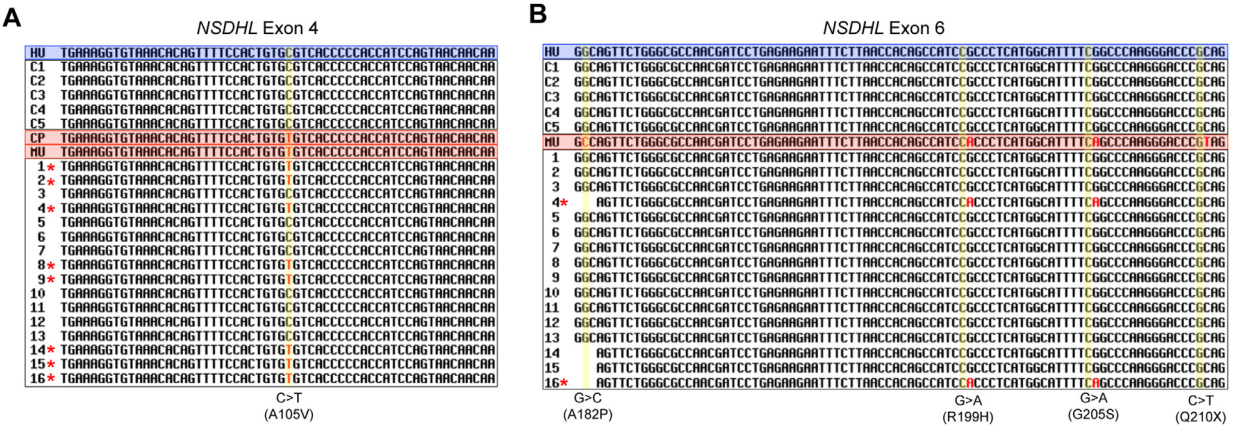

Fig. 4. Consensus sequence alignments for **(A)** *NSDHL* exon 4, and **(B)** *NSDHL* exon 6 in control (C1−C5) versus test (1−16) samples. The blue highlighted sequence *(HU)* represents the National Center for Biotechnology Information (NCBI) reference sequence for human *NSDHL* (NM_015922.2), and the red highlighted sequence *(MU)* represents all currently known mutations described for human *NSDHL* or a control sample that was spiked with the plasmid that contains the mutant *NSDHL* template *(CP)*. Red asterisks indicate the presence of mutation(s) in the test samples.

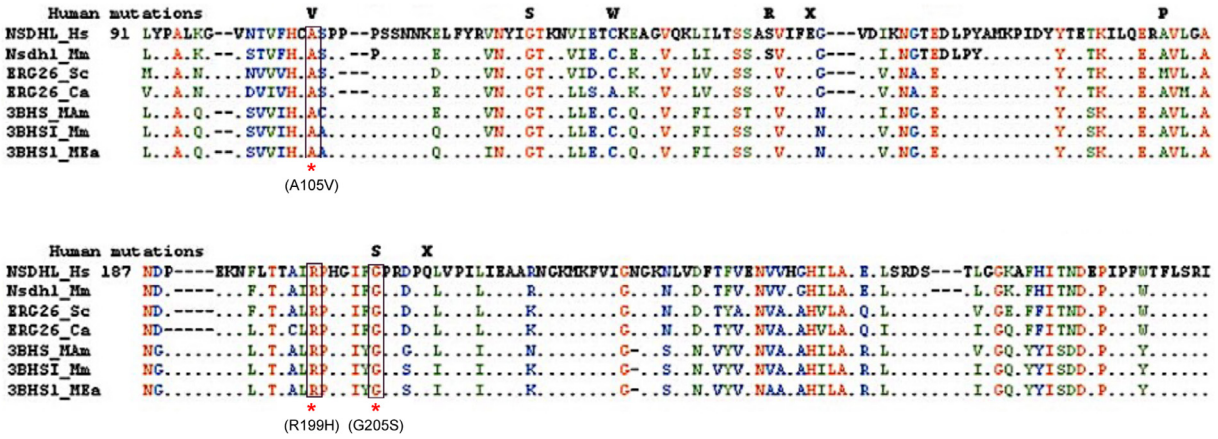

Fig. 5. Oral verruciform xanthoma (VX) mutations map to conserved amino acids. Sequence alignments between human *NSDHL* and homologues from multiple species reveal that the location of mutations of interest occurring preferentially within conserved residues (adapted from Bornholdt et al.[17]). From the top, in order: *Homo sapiens, Mus musculus, Saccharomyces cerevisiae, Candida albicans, Macaca mulatta, Mus musculus*, and *Mesocricetus auratus*. Identical amino acids are shown in red, observed mutations in black, strongly similar amino acids in green, and weak similarity in blue. Black dots represent nonconserved positions. Red asterisks denote mutations identified in this study.

previously associated with CHILD syndrome (A182P, Q210X) were not found.

A previous investigation compared the *NSDHL* gene from humans with similar functional genes from other species.[17] Compared with other functionally similar genes, point mutations present in *NSDHL* at codon positions 105, 182, 205, and 210 correspond to areas that are highly conserved and required for protein function (Figure 5). It is predicted that these genetic mutations influence NAD(P) binding within the active site of *NSDHL*. Although disruption of substrate binding does not necessarily eliminate catalytic activity, it will significantly reduce the catalytic efficiency of the enzyme. Without a properly functioning enzyme, metabolism could be disrupted in a cell. Therefore, it is predicted that these newly discovered mutations in the *NSDHL* gene contribute to a reduction in the enzymatic activity of the NSDHL protein, possibly explaining their role in a pathologic state.

CONCLUSIONS

In summary, we were able to demonstrate that missense mutations found in the *NSDHL* gene, which is known to be associated with CHILD syndrome, can be identified in oral VX lesions through DNA sequencing. Because we only selected specific exons for this study, to mirror a previous study that addressed cutaneous VX lesions, it is possible that additional exons of the *NSDHL* gene may harbor additional identified CHILD syndrome−associated mutations. Future studies should include sequencing of additional exons of the *NSDHL* gene. In addition, germline testing of affected individuals may be informative. Given that we were able to identify CHILD syndrome−associated mutations (and a previously reported somatic mutation unrelated to CHILD syndrome) in VX, there is evidence for an etiologic theory based on genetics for VX pathobiology.

ACKNOWLEDGMENTS

We wish to thank Cloe Twomey for supporting the chromatogram analyses performed in this study and members of the Amelio Lab for helpful suggestions during the preparation of this manuscript.

DISCLOSURE

This work was supported in part by the UNC Dental Foundation to A. L. Amelio and R. J. Padilla and by the University Cancer Research Fund to A. L. Amelio.

SUPPLEMENTARY MATERIALS

Supplementary material associated with this article can be found in the online version at doi:10.1016/j.oooo.2019.02.015.

REFERENCES

1. Shafer W. Verruciform xanthoma. *Oral Surg Oral Medicine Oral Pathology*. 1971;31:784-789.
2. Travis WD, Davis GE, Tsokos M, et al. Multifocal verruciform xanthoma of the upper aerodigestive tract in a child with a systemic lipid storage disease. *Am J Surg Pathol*. 1989;13:309-316.
3. Neville B. The verruciform xanthoma. A review and report of eight new cases. *Am J Dermatopathol*. 1986;8:247-253.
4. Philipsen HP, Reichart PA, Takata O. Verruciform xanthoma—biological profile of 282 oral lesions based on a literature survey with nine new cases from Japan. *Oral Oncol*. 2003;39:325-336.
5. Suhas S, Shekar CH, Sachin GP, et al. Verroucas xanthoma of faucial pillar—a case report. *Otolaryngol Open Access*. 2013;3:144. https://doi.org/10.4172/2161-119X.1000144. https://www.omicsonline.org/archive/ocr-volume-3-issue-4-year-2013.html https://www.omicsonline.org/verroucas-xanthoma-of-faucial-pillar-a-case-report-2161-119X.1000144.php?aid=21342.

6. Qi Y, Sun Q, Yang P, Song A. A case of multiple verruciform xanthoma in gingiva. *Br J Oral Maxillofac Surg*. 2014;52:e1-e3.
7. Shetty A, Nakhaei K, Lakkashetty Y, Mohseni M, Mohebatzadeh I. Oral verruciform xanthoma: a case report and literature review. *Case Reports Dent*. 2013;2013:528967.
8. Nowparast B, Howell F, Rick G. Verruciform xanthoma: a clinicopathologic review and report of fifty-four cases. *Oral Surg Oral Medicine Oral Pathol*. 1981;51:619-625.
9. Connolly SB, Lewis EJ, Lindholm JS, Zelickson BD, Zachary CB, Tope WD. Management of cutaneous verruciform xanthoma. *J Am Acad Dermatol*. 2000;42:343-347.
10. Mehra S, Li L, Fan C-YY, Smoller B, Morgan M, Somach S. A novel somatic mutation of the 3 beta-hydroxysteroid dehydrogenase gene in sporadic cutaneous verruciform xanthoma. *Arch Dermatol*. 2005;141:1263-1267.
11. Hu J-AA, Li Y, Li S. Verruciform xanthoma of the oral cavity: clinicopathological study relating to pathogenesis. Report of three cases. *APMIS*. 2005;113:629-634.
12. Khaskhely NM, Uezato H, Kamiyama T, et al. Association of human papillomavirus type 6 with a verruciform xanthoma. *Am J Dermatopathol*. 2000;22:447-452.
13. Zegarelli DJ, Zegarelli-Schmidt EC, Zegarelli EV. Verruciform xanthoma. Further light and electron microscopic studies, with the addition of a third case. *Oral Surg Oral Med Oral Pathol*. 1975;40:246-256.
14. Nathan C. Secretory products of macrophages. *J Clin Invest*. 1987;79:319-326.
15. Hummel M, Cunningham D, Mullett C, Kelley R, Herman G. Left-sided CHILD syndrome caused by a nonsense mutation in the *NSDHL* gene. *Am J Med Genet A*. 2003;122 A:246-251.
16. Xu X, Huang L, Wang Q, Sun J. Multiple verruciform xanthomas in the setting of congenital hemidysplasia with ichthyosiform erythroderma and limb defects syndrome. *Pediatr Dermatol*. 2015;32:135-137.
17. Bornholdt D, König A, Happle R, et al. Mutational spectrum of NSDHL in CHILD syndrome. *J Med Genet*. 2005;42:e17.
18. Ohashi M, Mizushima N, Kabeya Y, Yoshimori T. Localization of mammalian NAD(P)H steroid dehydrogenase-like protein on lipid droplets. *J Biol Chem*. 2003;278:36819-36829.
19. Deng X, Berletch JB, Nguyen DK, Disteche CM. X chromosome regulation: diverse patterns in development, tissues and disease. *Nat Rev Genet*. 2014;15:367-378.
20. Yu X, Zhang J, Gu Y, et al. CHILD syndrome mimicking verrucous nevus in a Chinese patient responded well to the topical therapy of compound of simvastatin and cholesterol. *J Eur Acad Dermatol*. 2018;32:1209-1213.
21. Hashimoto K, Prada S, Lopez AP, Hoyos JG, Escobar M. CHILD syndrome with linear eruptions, hypopigmented bands, and verruciform xanthoma. *Pediatr Dermatol*. 1998;15:360-366.

Reprint requests:

Antonio L. Amelio
University of North Carolina at Chapel Hill
Koury Oral Health Sciences Building
Room 3510, 385 South Columbia Street
CB#7455, Chapel Hill
NC 27599-7455
USA.
alamelio@email.unc.edu